STM JOURNALS

Research & Reviews: Journal of Physics
ISSN: 2278-2265 (Online), ISSN: 2347-9973 (Print)
Volume 9, Issue 1
www.stmjournals.com

Variable Mass of a Test Particle in Copenhagen Problem with Manev-Type Potential

Abdullah A. Ansari[1,*], Sada Nand Prasad[2], Mehtab Alam[3]

[1]Associate Professor, International Center for Advanced Interdisciplinary Research (ICAIR), Ratiya Marg, Sangam Vihar, New Delhi, India

[2]Assistant Professor, Acharya Narendra Dev College, University of Delhi, Govindpuri, New Delhi, India

[3]Research Scholar, International Center for Advanced Interdisciplinary Research (ICAIR), Ratiya Marg, Sangam Vihar, New Delhi, India

Abstract

This study deals the behavior of the motion of a test particle (third body) in the special case of the circular restricted three-body problem when the mass of the test particle varies according to Jeans law and also considered that the equal mass of the primaries generates the Manev-type potentials. This special case of a restricted problem is known as the Copenhagen problem. We derive the equations of motion of the test particle and then evaluate the Jacobian integral. We investigate numerically the equilibrium points, regions of possible motion and attracting domain. Finally, we examine the stability of the equilibrium points and found that some equilibrium points are stable while rests are unstable.

Keywords: *Copenhagen problem, Manev-type potential, variable mass, stability of equilibria*

****Author for Correspondence*** E-mail: icairndin@gmail.com, mehtabalam@live.com

INTRODUCTION

The restricted problem is a well-known problem either it is in two-body, three-body, four-body or N-body. Scientists are always looking towards the new approach in field of their research. One of these approaches is the Copenhagen problem in which two equal primaries are moving in circular orbits around their common centre of mass and are creating quasi-homogeneous potential; this is also known as Manev-type potential.

Many scientists studied this problem with a different approach. Benet *et al*. studied the Copenhagen problem in the restricted three-body problem with chaotic scattering [1]. Diacu studied the collision and ejection orbits in three-particle systems with homogeneous potential function [2]. Perdios studied the asymptotic orbits and many other properties in the Copenhagen problem [3, 4]. Roy and Steves have performed their investigations from Caledonian problem to the Copenhagen problem [5]. A different class of investigations on the photo-gravitational Copenhagen problem has been studied by Kalvouridis [6-9].

Papadakis *et al*. have investigated the properties of the motion of an infinitesimal body by using the Levi-Civita transformation in the photogravitational-Copenhagen problem [10]. On the other hand with the same quasi-homogeneous potential in the regular polygon problem of $N+1$ bodies have been investigated by Fakis and Kalvouridis [11, 12]; and also they have investigated the locations of equilibrium points, zero-velocity curves as well as motion of permitted regions over the variation of Jacobian constant.

Zotos has studied the behavior of the motion of the test particle with the effect of oblateness and also, he has illustrated the basins of attraction in the electromagnetic Copenhagen problem [13, 14]. He also has shown the relation between the Newton-Raphson basins of attraction and the corresponding number of iterations needed for obtaining the desired accuracy. Suraj *et al*. have unveiled the fractal

basins of convergence associated with the existed equilibrium points in the Copenhagen problem when the primaries are created quasi-homogeneous potential [15].

Many researchers have investigated the variable of mass, as well as the basins of attraction in the restricted problem [16-34].

The structure of this paper is as follows: In the next part, we present the equations of motion with Jacobian constant; then we have performed the numerical results such as equilibrium points, regions of motion and attracting domain associated with the corresponding equilibrium points; after that we have examined the stability of equilibrium points. The paper ends with the conclusion.

EQUATIONS OF MOTION

By considering the Copenhagen problem i.e. both the primaries have equal mass (m_1=m_2) and moving in circular orbits around their common center of mass which is taken as origin O. And also, we suppose that both the primaries create force fields with an inverse cube Manev-type perturbed term. The third test particle of mass m varies according to the Jeans law, which is moving in the space under the influence of other two bodies but not affecting them. We consider a synodic coordinate system OXYZ, Ox pointing towards m_1 and Oxy being the orbital plane of the primaries, coinciding with the inertial coordinate system OXYZ, and revolving with angular velocity $\omega = n\,k$ about the z-axis. Where n is the magnitude of ω. Let us assume that the total mass of the primaries and the distance between them be unity and the time is so chosen that the gravitational constant and the angular velocity of the system are unity. Figure 1 shows the geometric configuration of the Copenhagen problem.

The equations of motion of the third variable mass body, with dimensionless variables in the synodic coordinate system where the variation of mass of the test particle originates from one point and have zero momenta as:

$$\frac{\dot{m}}{m}(\dot{x} - y) + (\ddot{x} - 2\dot{y}) = \mathrm{U}_x,$$
$$\frac{\dot{m}}{m}(\dot{y} + x) + (\ddot{y} + 2\dot{x}) = \mathrm{U}_y,$$
$$\frac{\dot{m}}{m}\dot{z} + \ddot{z} = \mathrm{U}_z, \quad (1)$$

with

$$\mathrm{U} = \frac{1}{2}(x^2 + y^2) + \frac{1}{\Delta}\sum_{s=1}^{2}\left(\frac{1}{r_s} + \frac{e}{r_s^2}\right), \quad (2)$$

Where, the quantity $\Delta = (2 + 4\mathrm{e})$ and e is the parameter (For more detail see[12]).

Using Jean's law, $\frac{dm}{dt} = -\gamma_1 m^{\alpha}$, Where, γ_1 is a variation constant and $0.4 \leq \alpha \leq 4.4$, and Meshcherskii space-time transformations,

$$x = \gamma_2^{-p}u,\ y = \gamma_2^{-p}v,\ z = \gamma_2^{-p}w,\ dt = \gamma_2^{-p}d\tau.$$

Where, $\gamma_2 = \frac{m}{m_0}$, which will increase if mass will increase and decrease if mass will decrease. The components of velocity and acceleration can be presented by setting, $\alpha = 1, p = \frac{1}{2}, q = 0$, as:

$$\dot{x} = \gamma_2^{-\frac{1}{2}}\left(\dot{u} + \frac{\gamma_1}{2}u\right),\ \ddot{x} = \gamma_2^{-\frac{1}{2}}\left(\ddot{u} + \gamma_1\dot{u} + \frac{\gamma_1^2}{2}u\right),$$
$$\dot{y} = \gamma_2^{-\frac{1}{2}}\left(\dot{v} + \frac{\gamma_1}{2}v\right),\ \ddot{y} = \gamma_2^{-\frac{1}{2}}\left(\ddot{v} + \gamma_1\dot{v} + \frac{\gamma_1^2}{2}v\right),$$
$$\dot{z} = \gamma_2^{-\frac{1}{2}}\left(\dot{w} + \frac{\gamma_1}{2}w\right),\ \ddot{z} = \gamma_2^{-\frac{1}{2}}\left(\ddot{w} + \gamma_1\dot{w} + \frac{\gamma_1^2}{2}w\right),$$

and $\frac{d}{dt} = \frac{d}{d\tau}$.

And hence the equations of motion can be rewritten as:

$$\ddot{u} - 2\dot{v} = \Pi_u,$$
$$\ddot{v} + 2\dot{u} = \Pi_v,$$
$$\ddot{w} = \Pi_w. \quad (3)$$

with, $\Pi = \frac{1}{2}(u^2 + v^2) + \frac{\gamma_1^2}{8}(u^2 + v^2 + w^2) + \frac{1}{\Delta}\sum_{s=1}^{2}\left(\frac{\gamma_2^{\frac{3}{2}}}{r_s} + \frac{\gamma_2^2 e}{r_s^2}\right)$, (4)

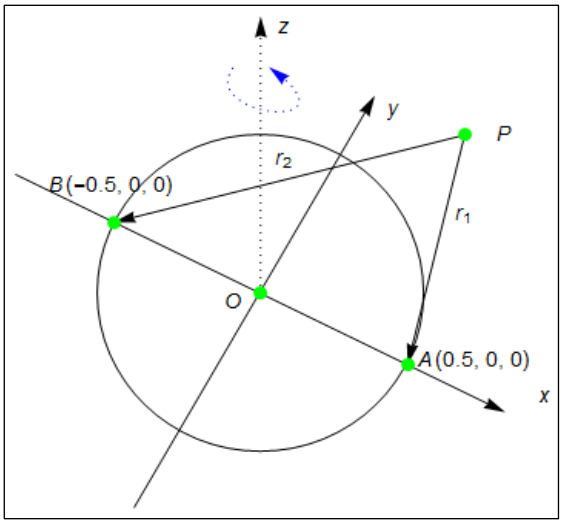

Fig. 1: *Geometric Configuration of the Copenhagen Problem.*

and $r_s^2 = (u \mp \frac{\sqrt{\gamma_2}}{2})^2 + v^2 + w^2$.

Therefore, Jacobian integral can be written as:

$$\dot{u}^2 + \dot{v}^2 + \dot{w}^2 = 2\Pi - C - 2\int_{t_0}^{t} \frac{\partial \Pi}{\partial t} dt, \quad (5)$$

Where, C is the Jacobian constant.

NUMERICAL RESULTS

Points of Equilibria

We have shown the locations of equilibrium points by solving numerically to the following equations:

$$\Pi_u = \Pi_v = \Pi_w = 0, \quad (6)$$

and are given in the Figure 2(a-d) corresponding to the value of *e*=-0.46, -0.26, 0.26 and 0.46 respectively.

At *e*=-0.46 in Figure 2(a), we found 13 equilibrium points in which five are collinear $L_{1, 2, 3, 4, 5}$ and eight are non-collinear $L_{6, 7, 8, 9, 10, 11, 12, 13}$. And also L_1 is at the origin, $L_{2, 4}$ and $L_{3, 5}$ are symmetrical about ordinate while $L_{6, 8, 10, 12}$ and $L_{7, 9, 11, 13}$ are symmetrical about abscissa respectively. At *e*=-0.26 in Figure 2(b), we found nine equilibrium points in which five equilibrium points $L_{1, 2, 3, 8, 9}$ lie on the ordinate and four equilibrium points ($L_{4, 5, 6, 7}$) are non-collinear where we observed that the equilibrium points ($L_{2, 4, 6, 8}$) and the equilibrium points ($L_{3, 5, 7, 9}$) are symmetrical with abscissa respectively. At *e*=0.26, 0.46 in Figure 2(c and d), we found five equilibrium points ($L_{1, 2, 3, 4, 5}$) in which three are on abscissa ($L_{1, 2, 3}$) and two are on ordinate ($L_{4, 5}$) where we observed that L_1 is at the origin, L_2

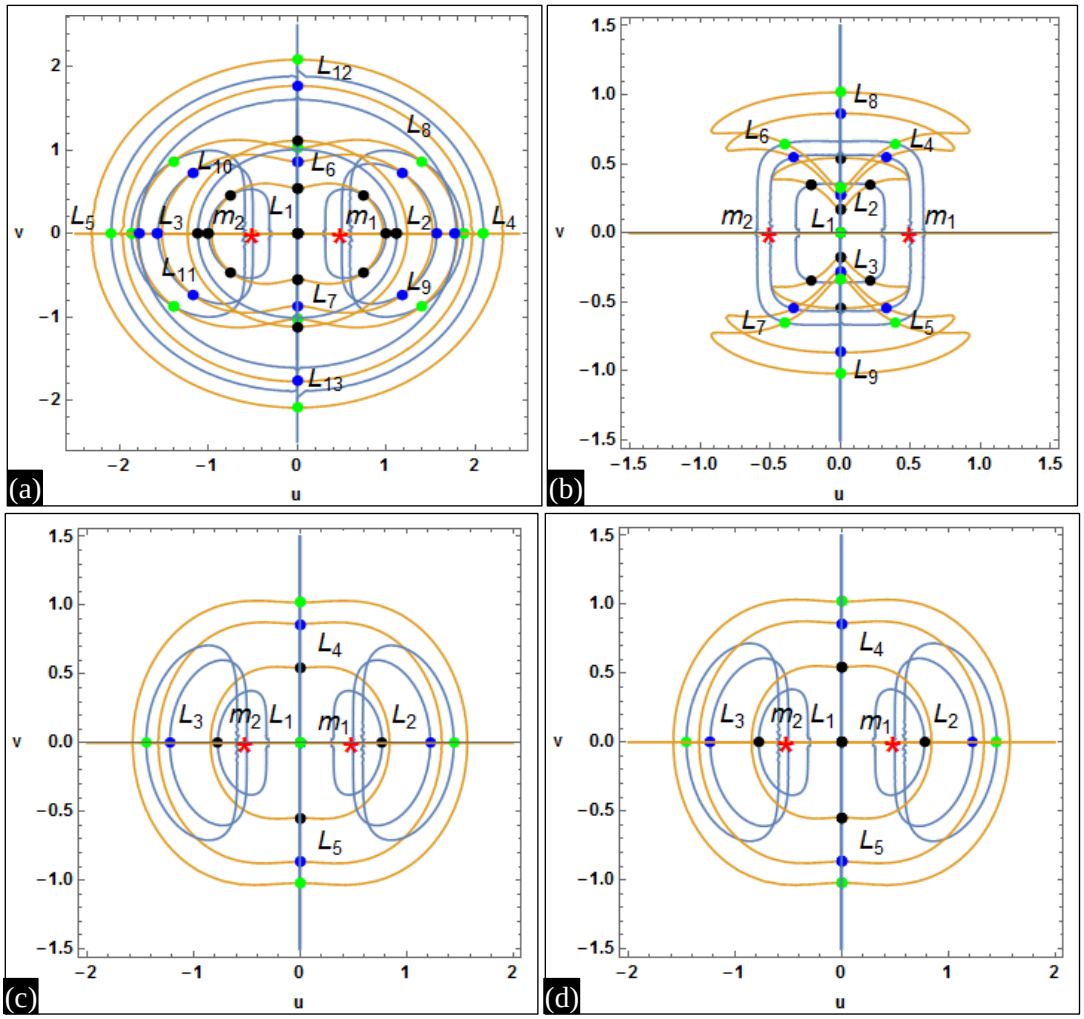

Fig. 2: *Locations of Equilibrium Points Black (γ_2=0.4), Blue (γ_2=1) and Green (γ_2=1.4) in u-v-Plane. Red Stars Denote the Locations of the Primaries. (a) Locations of Equilibrium Points at e=-0.46, (b) Locations of Equilibrium Points at e=-0.26, (c) Locations of Equilibrium points at e=0.26, (d) Locations of Equilibrium points at e=0.46*

and L_3 are symmetrical about ordinate while L_4 and L_5 are symmetrical about abscissa. In all these cases when we increase the value of variation constant γ_2=0.4 (Black), 1 (Blue), 1.4 (Green)), we observed that equilibrium points are moving away from the origin. Two red stars are representing the location of the primaries m_1 and m_2.

Regions of Possible Motion

To obtain the regions of possible or forbidden motion, we follow the procedure and terminology used by Ansari [22, 23]. Firstly, we have evaluated each value of Jacobian constant corresponding to the each equilibrium point and then we have plotted the regions of motion with the help of Eq. (5) and performed light blue shaded regions as the forbidden regions as given in Figure 3(a-f). This reveals very important dynamical properties of the motion of the test particle. Figure 3(a) represents the region corresponding to the equilibrium point L_1 and shows that test particle can neither move near both the primaries and around L_1. Figure 3(b) represents the region corresponding to the equilibrium points $L_{2, 3}$ and shows that the test particle can move near the equilibrium points $L_{6, 7}$. Figure 3(c) represents the region corresponding to the equilibrium points $L_{4, 5}$ and shows that the test particle can move near the equilibrium points $L_{2, 3, 4, 5, 6, 7}$. Figure 3(d) represents the region corresponding to the equilibrium points $L_{6, 7}$ and shows that the test particle can neither move near equilibrium points nor near both the primaries. Figure 3(e) represents the region corresponding to the equilibrium points $L_{8, 9, 10, 11}$ and shows that the test particle can move near the equilibrium points $L_{2, 3, 4, 5, 6, 7}$. This is similar to the Figure 3(c) but in this case the areas of the regions are more than the area given in Figure 3(c). Figure 3(f) represents the region corresponding to the equilibrium points $L_{12, 13}$ and shows that the test particle can neither move near the equilibrium point L_1 nor near both the primaries. Green points are showing the positions of the equilibrium points and red stars are presenting the locations of both the primaries.

Attracting Domain

To study the attractive domain of the test particle, we use simple, fast and accurate Newton-Raphson iterative method. The attracting domains are composed by all the initial values that tend to a specific attracting point which is one of the equilibrium points. The attracting domain shows the most important qualitative behavior of the dynamical systems.

Using the above iterative method, we have drawn the attracting domain in u-v-plane for variation constants γ_1=0.2 and γ_2=1.4. The algorithm of our problem is as follows:

$$u_{n+1} = u_n - \left(\frac{\Pi_u\Pi_{vv} - \Pi_v\Pi_{uv}}{\Pi_{uu}\Pi_{vv} - \Pi_{uv}\Pi_{vu}}\right)_{(u_n, v_n)}, \quad (7)$$

$$v_{n+1} = v_n - \left(\frac{\Pi_v\Pi_{uu} - \Pi_u\Pi_{vu}}{\Pi_{uu}\Pi_{vv} - \Pi_{uv}\Pi_{vu}}\right)_{(u_n, v_n)}, \quad (8)$$

Where, u_n, v_n are the values of u and v coordinates of the n^{th} step of the Newton-Raphson iterative process. If the initial point converges rapidly to one of the equilibrium points then this point (u, v) will be a member of the attracting domain. This process stops when the successive approximation converges to an equilibrium point. We also need to clear that the attracting domain is not related with the classical attracting domain in dissipative system. For the classification of different equilibrium points on the plane, we used a color code.

We have drawn the attracting domain for *e*=-0.46 in u-v-plane and given in Figure 4(a). For more clear view, we have drawn the zoomed part of Figure 4(a) and we observed that there are 13 attracting points $L_{1, 2, 3, 4, 5, 6, 7, 8, 9, 10, 11, 12, 13}$. From the Figure 4b, we found that $L_{1, 2, 3, 4, 5}$ correspond to the cyan color region which is extended to infinity, L_6 corresponds to the light purple color region which is finite, $L_{8, 10}$ corresponds to the blue color region which is finite, $L_{7, 9, 11}$ corresponds to the green color region which is finite, $L_{12, 13}$ corresponds to the red color region which is extended to infinity.

Also, we have drawn the attracting domain for *e*=-0.26 in u-v-plane and given in Figure 5(a). The zoomed part of Figure 5(a) is Figure 5(b), we found nine attracting points $L_{1, 2, 3, 4, 5, 6, 7, 8, 9}$. We observed from this figure that L_1 corresponds to the cyan color region which is finite, $L_{2, 4, 6}$ correspond to the blue color region which is extended to infinity, $L_{3, 5, 7}$ correspond to the green color region which is

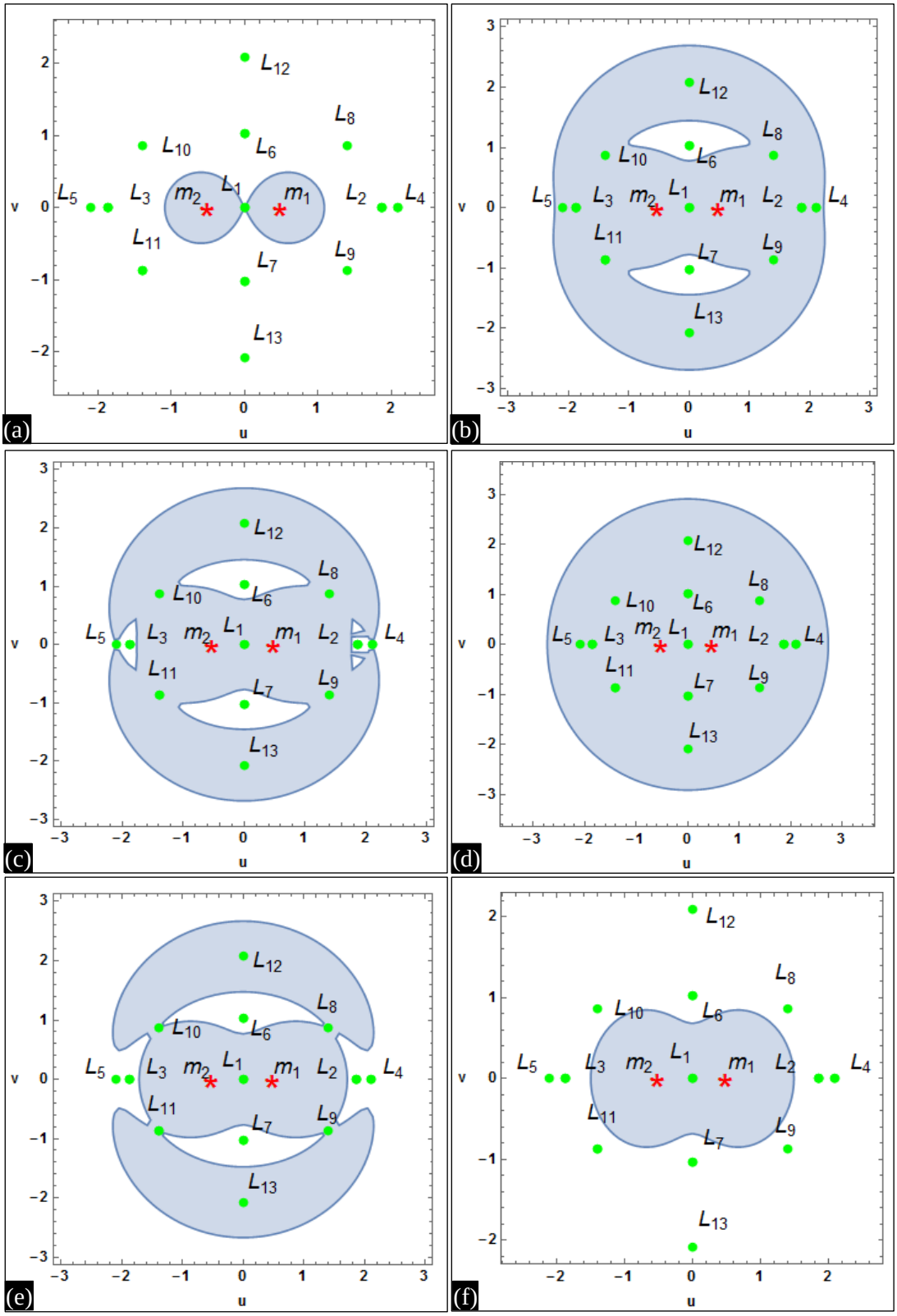

Fig. 3: *Regions of Possible Motion at γ_1=0.2, γ_2=1.4 and e=-0.46 in u-v-Plane. Red Stars Denote the Locations of the Primaries. (a) At C=5.5999999999 corresponding to L_1, (b) At C=19.3848426185 corresponding to $L_{2,3}$, (c) At C=19.3654584658 corresponding to $L_{4,5}$ (d) At C=19.9605165382 corresponding to $L_{6,7}$, (e) At C=19.3302266455 corresponding to $L_{8,9,10,11}$ (f) At C=18.6999367528 corresponding to $L_{12,13}$*

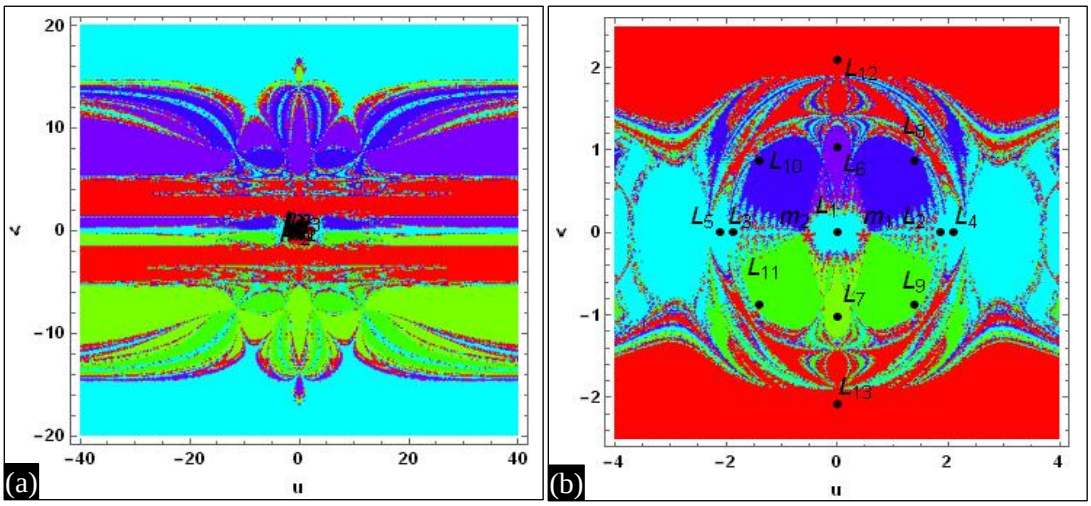

Fig. 4: *Attracting Domain for γ_1=0.2 and γ_2=1.4 in u-v- Plane. Red Stars Denote the Locations of the Primaries. (a). Attracting Domain at e = - 0.46, (b) Zoomed Part of Figure a Near Primaries*

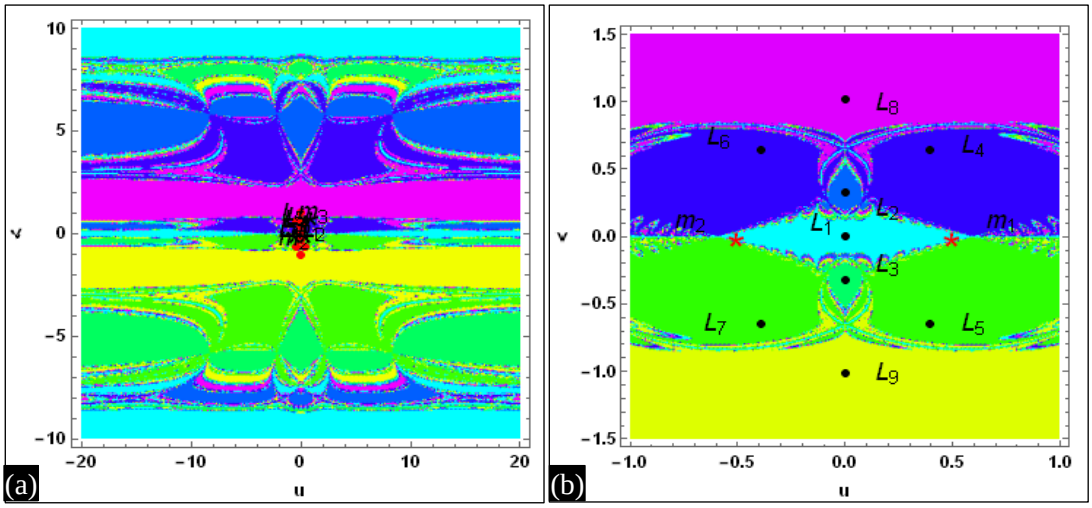

Fig. 5: *Attracting Domain for γ_1=0.2 and γ_2=1.4 in u-v-Plane. Red Stars Denote the Locations of the Primaries. (a). Attracting Domain at e= 0.26, (b). Zoomed Part of Figure (a) Near Primaries*

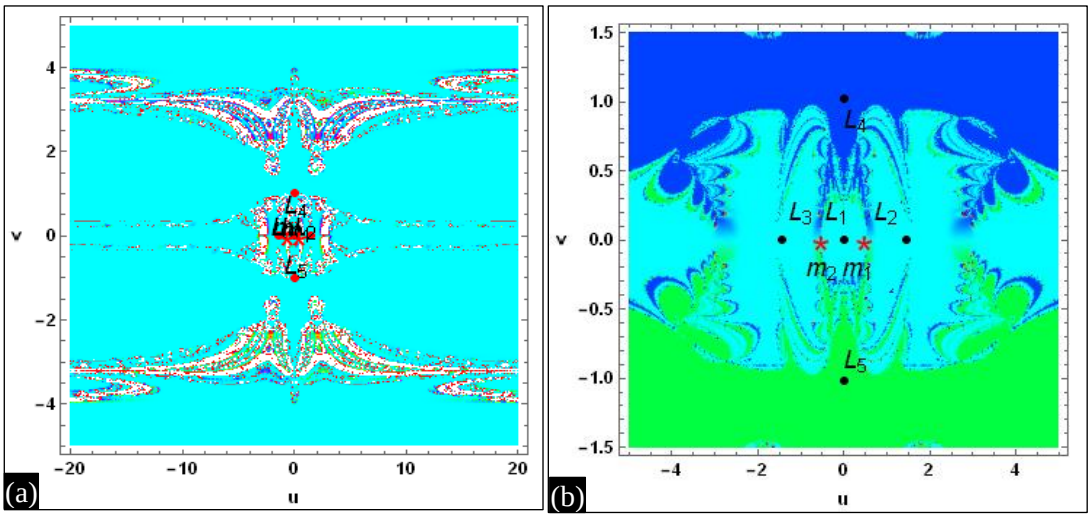

Fig. 6: *Attracting Domain for γ_1=0.2 and γ_2=1.4 in u-v-Plane. Red Stars Denote the Locations of the Primaries. (a). Attracting Domain at e=0.26, (b). Zoomed Part of Figure (a) Near Primaries*

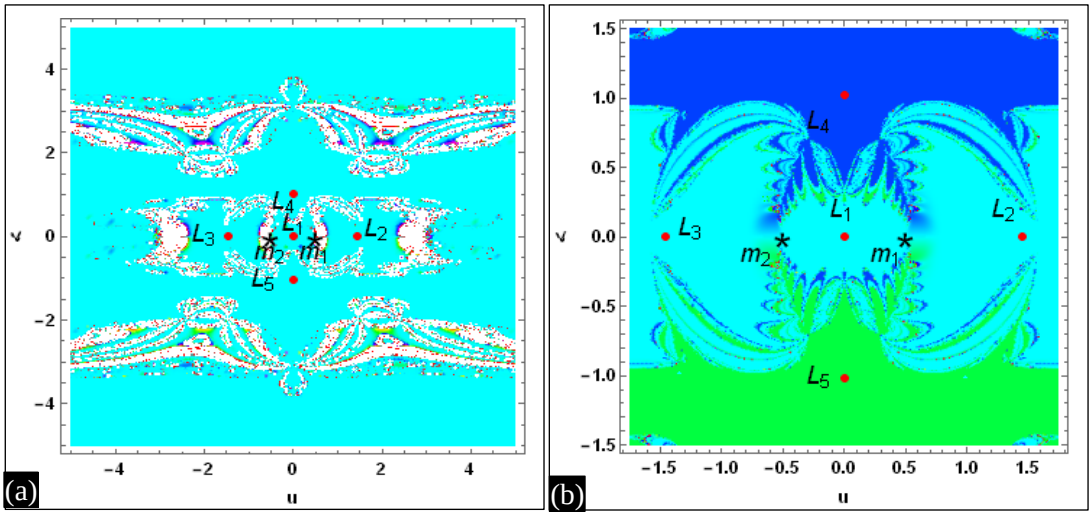

Fig. 7: *Attracting Domain for γ_1=0.2 and γ_2=1.4 in u-v-Plane. Black Stars Denote the Locations of the Primaries. (a). Attracting Domain at e = 0.46, (b). Zoomed Part of Figure (a) Near Primaries*

extended to infinity, L_8 corresponds to the purple color region which is extended to infinity and L_9 corresponds to the yellow color region which is extended to infinity.

Further we have drawn the attracting domain for *e*=0.26 and 0.46 in u-v-plane and given in Figure 6(a) and 7(a) respectively. The zoomed part of Figure 6(a) is Figure 6(b) and Figure 7(a) is Figure 7(b), in both the cases we found five attracting points $L_{1, 2, 3, 4, 5}$. We observed from these figures that $L_{1, 2, 3}$ correspond to the cyan color region which is extended to infinity, L_4 corresponds to the blue color region which is extended to infinity and L_5 correspond to the green color region which is also extended to infinity. In all the figures red stars are presenting the locations of the primaries. Similarly, we can determine the attracting domain for the other values of the variation constants.

Stability

To examine the stability of an equilibrium point (u_0, v_0, w_0), we displace the test particle from the point (u_0, v_0, w_0) to $(u_0 + \xi, v_0 + \eta, w_0 + \zeta)$. Substituting these values in system (3), we get the variational equations:

$$\begin{aligned}
\ddot{\xi} - 2\dot{\eta} &= \Pi^0_{uu}\xi + \Pi^0_{uv}\eta + \Pi^0_{uw}\zeta,\\
\ddot{\eta} + 2\dot{\xi} &= \Pi^0_{vu}\xi + \Pi^0_{vv}\eta + \Pi^0_{vw}\zeta,\\
\ddot{\zeta} &= \Pi^0_{wu}\xi + \Pi^0_{wv}\eta + \Pi^0_{ww}\zeta.
\end{aligned} \tag{9}$$

Where (ξ, η, ζ) are small displacements given in the coordinates of the equilibrium point. The superscript 0 indicates the value at (u_0, v_0, w_0).

In the phase space, the above system can be rewritten as:

$$\begin{aligned}
&\dot{\xi} = \xi_1, \dot{\eta} = \eta_1, \dot{\zeta} = \zeta_1\\
&\dot{\xi}_1 = \Pi^0_{uu}\xi + \Pi^0_{uv}\eta + \Pi^0_{uw}\zeta + 2\eta_1,\\
&\dot{\eta}_1 = \Pi^0_{vu}\xi + \Pi^0_{vv}\eta + \Pi^0_{vw}\zeta - 2\xi_1,\\
&\dot{\zeta}_1 = \Pi^0_{wu}\xi + \Pi^0_{wv}\eta + \Pi^0_{ww}\zeta.
\end{aligned} \tag{10}$$

Due to variation of mass and distance with time, we use the Meshcherskii space-time inverse transformations to examine the stability of the equilibrium points.

$$\begin{aligned}
&\xi_2 = \gamma_2^{-1/2}\xi, \eta_2 = \gamma_2^{-1/2}\eta, \zeta_2 = \gamma_2^{-1/2}\zeta,\\
&\xi_3 = \gamma_2^{-1/2}\xi_1, \eta_3 = \gamma_2^{-1/2}\eta_1, \zeta_3 = \gamma_2^{-1/2}\zeta_1.
\end{aligned} \tag{11}$$

The system (13) can be written as follows:

$$\dot{X} = BX, \tag{12}$$

Where,

$$\dot{X} = \begin{pmatrix} \dot{\xi}_2 \\ \dot{\eta}_2 \\ \dot{\zeta}_2 \\ \dot{\xi}_3 \\ \dot{\eta}_3 \\ \dot{\zeta}_3 \end{pmatrix}, X = \begin{pmatrix} \xi_2 \\ \beta_2 \\ \gamma_2 \\ \xi_3 \\ \eta_3 \\ \zeta_3 \end{pmatrix}$$

and $B = \begin{pmatrix} \frac{1}{2}\gamma_1 & 0 & 0 & 1 & 0 & 0 \\ 0 & \frac{1}{2}\gamma_1 & 0 & 0 & 1 & 0 \\ 0 & 0 & \frac{1}{2}\gamma_1 & 0 & 0 & 1 \\ \Pi^0_{uu} & \Pi^0_{uv} & \Pi^0_{uw} & \frac{1}{2}\gamma_1 & 2 & 0 \\ \Pi^0_{vu} & \Pi^0_{vv} & \Pi^0_{vw} & -2 & \frac{1}{2}\gamma_1 & 0 \\ \Pi^0_{wu} & \Pi^0_{wv} & \Pi^0_{ww} & 0 & 0 & \frac{1}{2}\gamma_1 \end{pmatrix}$ (13)

The stability of the system depends on the boundedness of the solution of linear and homogenous system of Eq. (14). The characteristic equation for the matrix B is:

$$\lambda^6 + \alpha_5\lambda^5 + \alpha_4\lambda^4 + \alpha_3\lambda^3 + \alpha_2\lambda^2 + \alpha_1\lambda + \alpha_0 = 0, \quad (14)$$

Where,

$$\alpha_0 = \Pi^0_{uw}\Pi^0_{vv}\Pi^0_{wu} - 2\Pi^0_{uv}\Pi^0_{vw}\Pi^0_{wu} + \Pi^0_{uu}\Pi^0_{vw}\Pi^0_{wv} + \Pi^0_{uv}\Pi^0_{vu}\Pi^0_{ww} - \Pi^0_{uu}\Pi^0_{vv}\Pi^0_{ww} + \frac{1}{4}\gamma_1^4(\Pi^0_{uu}\Pi^0_{vv} - \Pi^0_{uv}\Pi^0_{vu} - \Pi^0_{uw}\Pi^0_{wu} - \Pi^0_{vw}\Pi^0_{wv} + \Pi^0_{uu}\Pi^0_{ww} - 4\Pi^0_{ww} + \Pi^0_{vv}\Pi^0_{ww}) - \frac{1}{64}\gamma_1^2(4\Pi^0_{uu} + 4\Pi^0_{vv} + 4\Pi^0_{ww} - \gamma_1^2 - 16)$$

$$\alpha_1 = (\Pi^0_{uv}\Pi^0_{vu} + \Pi^0_{uw}\Pi^0_{wu} - \Pi^0_{uu}\Pi^0_{vv} - \Pi^0_{uu}\Pi^0_{ww} - \Pi^0_{vv}\Pi^0_{ww} + 4\Pi^0_{ww} + \Pi^0_{vw}\Pi^0_{wv})\gamma_1 - \frac{1}{64}\gamma_1^3(8\Pi^0_{uu} + 8\Pi^0_{vv} + 8\Pi^0_{ww} - 3\gamma_1^2 - 32)$$

$$\alpha_2 = \Pi^0_{uu}\Pi^0_{vv} - \Pi^0_{uv}\Pi^0_{vu} - \Pi^0_{uw}\Pi^0_{wu} - \Pi^0_{vw}\Pi^0_{wv} - 4\Pi^0_{ww} + \Pi^0_{uu}\Pi^0_{ww} - \frac{3}{2}\gamma_1^2\left(\Pi^0_{uu} + \Pi^0_{vv} + \Pi^0_{ww} - \frac{5}{8}\gamma_1^2 - 6\right)$$

$$\alpha_3 = 2\left(\Pi^0_{uu} + \Pi^0_{vv} + \Pi^0_{ww} - \frac{5}{4}\gamma_1^2 - 4\right)\gamma_1$$

$$\alpha_4 = 4 - \Pi^0_{uu} - \Pi^0_{vv} - \Pi^0_{ww} + \frac{15}{4}\gamma_1^2$$

$$\alpha_5 = -3\,\gamma_1$$

We have solved Eq. (14) numerically corresponding to four different values of parameter *e* (-0.46, -0.26, 0.26, 0.46) and evaluated characteristic roots are given in Tables 1-4. We observed from the Table 1 which corresponds to the value at *e*=-0.46 that five equilibrium points are unstable because at-least one characteristic root is either positive real number or positive real part of the complex characteristic root, while other eight equilibrium points are stable due to having all purely imaginary roots. From the Table 2 which corresponds to the value at *e*=-0.26, we found that five equilibrium points are unstable while four equilibrium points are stable. Further from the Tables 3 and 4 which correspond to the values *e*=0.26 and 0.46 respectively, we got that all the equilibrium points are unstable. These results of our finding confirm that *e* should be less than zero to get the stable parking points for the test particle.

Table 1: *Corresponding Characteristic Roots of Equilibria in u-v-Plane at γ_1=0.2, γ_2=1.4 and e=-0.46.*

Equilibrium Point	Roots	Nature
(0.0000000000, 0.0000000000)	±4.6222946067 *i*, ±0.8225975119, ±1.1771182743	Unstable
(±1.8661426980, 0.000000000)	± 0.7128992372i, ±1.1250321578i, ±0.7921506876i	Stable
(±2.0963161056, 0.0000000000)	±0.5982444741 i, ±0.9765146781i, ±0.1838752208	Unstable
(0.000000000, ±1.0263110938)	±0.6614947987i, ±0.9938485033i, ±1.2739355368 i	Stable
(±1.396610712, ±0.8690713779)	±0.6875361929 i, ±0.7809442064i, ±1.2142581299i	Stable
(0.0000000000, ±2.0876538555)	±0.9915264737i, ±0.2573703282, ±0.4816771322i	Unstable

Table 2: *Corresponding Characteristic Roots of Equilibria in u-v-Plane at γ_1=0.2, γ_2=1.4 and e=-0.26.*

Equilibrium Point	Roots	Nature
0.0000000000, 0.0000000000	±4.6222946067i, ±0.8225975119, ±1.1771182743	Unstable
0.0000000000, ±0.3283292599	±0.9428538547 i, ±1.0000000000i, ±3.1956775970i	Stable
±0.392022467, ±0.6465026888	±2.6526461445i, ±0.9999999999i, ±0.6691780295	Unstable
(0.000000000, ±1.0175925411)	±0.6500888042 i, ±1.0000000000 i, ±1.2858928870 i	Stable

Table 3: *Corresponding Characteristic Roots of Equilibria in u-v-Plane at γ_1=0.2, γ_2=1.4 and e=0.26.*

Equilibrium Point	Roots	Nature
(0.0000000000, 0.0000000000)	±3.2931444341 I, ±3.2751858123i, ±5.0075269924	Unstable
(±1.4448459424, 0.000000000)	±1.2238908177i, ±1.2596712479i, ±1.4103990903	Unstable
(0.000000000, ±1.0206317950)	±0.9400690878 i, ±0.9999999999i, ±0.8006681496	Unstable

Table 4: *Corresponding Characteristic Roots of Equilibria in u-v-Plane at γ_1=0.2, γ_2=1.4 and e=0.46.*

Equilibrium Point	Roots	Nature
(0.0000000000, 0.0000000000)	±3.4385074281i, ±3.4495137536i, ±5.4239418448	Unstable
(±1.454312381, 0.0000000000)	±1.2238908177i, ±1.2596712479i, ±1.4103990903	Unstable
(0.000000000, ±1.0207917243)	±0.9400690878i, ±0.9999999999i, ±0.8006681496	Unstable

CONCLUSION

Here we have studied the effect of variation of mass in the Copenhagen problem where primaries are creating quasi-homogeneous potential which is also known as Manev-type potential. We have derived the equations of motion which is different from Fakis [12] by the variation parameters γ_1 and γ_2. And then we have evaluated the quasi-Jacobian constant. Followed from this, we have evaluated numerically the equilibrium points for the four values of the parameter *e*=-0.46, -0.26, 0.26 and 0.46 and got thirteen, nine, five and five equilibrium points (Figure 2(a-d) respectively. These equilibrium points are also found like Fakis, when the variation constants are absent [12]. Following the procedure given in Ansari [22, 23], we have drawn the regions of motion for four values of *e* (Figure 3(a-f). Further, we have illustrated the Newton-Raphson attracting domain for the same four values of e; these are shown in Figures (4a, b), (5a, b), (6a, b) and (7a, b). Finally we have evaluated the characteristic roots corresponding to each equilibrium points and written in the Tables 1-4, and from here we observed that some equilibrium points are unstable because at least one root is positive real value or positive real part of the complex roots while some are stable. In this way we observed that the variation parameters γ_1, γ_2 and *e* have great impact on the motion of the test particle.

REFERENCES

1. Benet L, Trautmann D, Seligman TH. Chaotic Scattering in the Restricted Three-Body Problem I. The Copenhagen Problem. *Celest Mech Dyn Astr*. 1996; 66(2): 203-228p.
2. Diacu FN. Near-Collision Dynamics for Particle Systems with Quasi Homogeneous Potentials. *J Differ Equations*. 1996; 128(1): 58-77p.
3. Perdios EA. Asymptotic Orbits and Terminations of Families in the Copenhagen Problem. *Astrophys Space Sci*. 1996; 240(1): 141-152p.
4. Perdios EA. Asymptotic Orbits and Terminations of Families in the Copenhagen Problem, II. *Astrophys Space Sci*. 1997; 254(1): 61-66p.
5. Roy AE, Steves BA. Some Special Restricted Four-Body Problems-II. From Caledonia to Copenhagen. *Planet Space Sci*. 1998; 46(11-12): 1475-1486p.

6. Kalvouridis TJ. On a Class of Equilibria of a Small Rigid Body in a Copenhagen Configuration. *Rom Astron J*. 2008a; 18(2): 167–179p.
7. Kalvouridis TJ. On Some New Aspects of the Photo-Gravitational Copenhagen Problem. *Astrophys Space Sci*. 2008b; 317(1-2): 107-117p.
8. Kalvouridis TJ. Bifurcations in the Topology of Zero-Velocity Surfaces in the Photo-Gravitational Copenhagen Problem. *Int J Bifurcat Chaos*. 2009; 19(03): 1097-1111p.
9. Kalvouridis TJ, Gousidou-Koutita MC. Basins of Attraction in the Copenhagen Problem Where the Primaries are Magnetic Dipoles. *Appl Math*. 2012; 3(6): 541–548p.
10. Papadakis K, Ragos O, Litzerinos C. Asymmetric Periodic Orbits in the Photogravitational Copenhagen Problem. *J Comput Appl Math*. 2009; 227(1): 102-114p.
11. Fakis DG, Kalvouridis TJ. On a Property of the Zero-Velocity Curves in the Regular Polygon Problem of N+1 Bodies with a Quasi-Homogeneous Potential. *Rom Astron J*. 2014; 24(1): 7-26p.
12. Fakis D, Kalvouridis T. The Copenhagen Problem with a Quasi-Homogeneous Potential. *Astrophys Space Sci*. 2017; 362(5): 102p.
13. Zotos EE. Crash Test for the Copenhagen Problem with Oblateness. *Celest Mech Dyn Astron*. 2015; 122(1): 75-99p.
14. Zotos EE. Determining the Newton-Raphson Basins of Attraction in the Electromagnetic Copenhagen Problem. *Int J Non-Lin Mech*. 2017; 90: 111-123p.
15. Suraj MS, Zotos EE, Kaur C, Aggarwal R, Mittal A. Fractal Basins of Convergence of Libration Points in the Planar Copenhagen Problem with a Repulsive Quasi-Homogeneous Manev-Type Potential. *Int J Non-Lin Mech*. 2018; 103: 113-127p.
16. Abouelmagd EI, Mostafa A. Out of Plane Equilibrium Points Locations and the Forbidden Movement Regions in the Restricted Three-Body Problem with Variable Mass. *Astrophys Space Sci*. 2015; 357(1): 58p.
17. Abouelmagd EI, Ansari AA. The Motion Properties of the Infinitesimal Body in the Framework of Bicircular Sun Perturbed Earth–Moon System. *New Astron*. 2019; 73: 101282p.
18. Ansari AA. Stability of the Equilibrium Points in the Circular Restricted Four Body Problem with Oblate Primary and Variable Mass. *Int J Adv Astron*. 2016a; 4(1): 14-19p.
19. Ansari AA. The Photo Gravitational Circular Restricted Four-Body Problem with Variable Masses. *J Eng Appl Sci*. 2016b; 3(2): 30-38p.
20. Ansari AA. The Circular Restricted Four-Body Problem with Variable Masses. *Nonlinear Sci Lett A*. 2017a; 8(3): 303-312p.
21. Ansari AA. Effect of Albedo on the Motion of the Infinitesimal Body in Circular Restricted Three-Body Problem with Variable Masses. *Ital J Pure Appl Math*. 2017b; 38: 581-600p.
22. Ansari AA, Alhussain ZA, Prasad SN. Circular Restricted Three-Body Problem When Both the Primaries are Heterogeneous Spheroid of Three Layers and Infinitesimal Body Varies Its Mass. *J Astrophys Astron*. 2018a; 39(5): 57p.
23. Ansari AA. The Circular Restricted Four-body Problem with Triaxial Primaries and Variable Infinitesimal Mass. *Applications & Applied Mathematics (AAM)*. 2018b; 13(2): 818-838p.
24. Ansari AA, Kellil R, Alhussain ZA. Behavior of an Infinitesimal-Variable-Mass Body in CR3BP; the Primaries are Finite Straight Segments. *Punjab Univ J Math*. 2019a; 51(5): 107-120p.
25. Ansari AA, Kellil R, Al-Hussain ZA, Ul-Haq W. Effect of Variation of Charge in the Circular Restricted Three-Body Problem with Variable Masses. *J Taibah Univ Sci*. 2019b; 13(1): 670-677p.
26. Ansari AA, Ali A, Alam M, Kellil R. Cyclic Kite Configuration with Variable Mass of the Fifth Body in R5BP. *Applications & Applied Mathematics (AAM)*. 2019c; 14(2): 985-1002p.
27. Jeans J. *Astronomy and Cosmogony*. CUP (Cambridge University Press) Archive; 1929.

28. Luk'yanov LG. On the Restricted Circular Conservative Three-Body Problem with Variable Masses. *Astron Lett*. 2009; 35(5): 349-359p.
29. Meshcherskii IV. *Works on the Mechanics of Bodies of Variable Mass*. Moscow: GITTL; 1949.
30. Shrivastava AK, Ishwar B. Equations of Motion of the Restricted Problem of Three Bodies with Variable Mass. *Celestial Mechanics*. 1983; 30(3): 323-328p.
31. Singh J, Ishwar B. Effect of Peturbations on the Location of Equilibrium Points in the Restricted Problem of Three Bodies with Variable Mass. *Celestial Mechanics*. 1984; 32(4): 297-305p.
32. Singh J, Ishwar B. Effect of Perturbations on the Stability of Triangular Points in the Restricted Problem of Three Bodies with Variable Mass. *Celestial Mechanics*. 1985; 35(3): 201-207p.
33. Singh J, Leke O. Existence and Stability of Equilibrium Points in the Robe's Restricted Three-Body Problem with Variable Masses. *International Journal of Astronomy and Astrophysics (IJAA)*. 2013; 3(2): 113-122p.
34. Zhang MJ, Zhao CY, Xiong YQ. On the Triangular Libration Points in Photogravitational Restricted Three-Body Problem with Variable Mass. *Astrophys Space Sci*. 2012; 337(1): 107-113p.

Cite this Article
Abdullah A. Ansari, Sada Nand Prasad, Mehtab Alam. Variable Mass of a Test Particle in Copenhagen Problem with Manev-Type Potential. *Research & Reviews: Journal of Physics*. 2020; 9(1): 17–27p.